Uncovering the genetic blueprint of the *C. elegans* nervous system

István A. Kovács[a,b,c,d] (iD), Dániel L. Barabási[e] (iD), and Albert-László Barabási[b,c,f,1] (iD)

[a]Department of Physics and Astronomy, Northwestern University, Evanston, IL 60208; [b]Department of Data and Network Science, Central European University, Budapest 1051, Hungary; [c]Network Science Institute, Northeastern University, Boston, MA 02115; [d]Wigner Research Centre for Physics, Institute for Solid State Physics and Optics, Budapest 1121, Hungary; [e]Biophysics Program, Harvard University, Cambridge, MA 02138; and [f]Department of Medicine, Brigham and Women's Hospital, Harvard Medical School, Boston, MA 02115

Despite rapid advances in connectome mapping and neuronal genetics, we lack theoretical and computational tools to unveil, in an experimentally testable fashion, the genetic mechanisms that govern neuronal wiring. Here we introduce a computational framework to link the adjacency matrix of a connectome to the expression patterns of its neurons, helping us uncover a set of genetic rules that govern the interactions between neurons in contact. The method incorporates the biological realities of the system, accounting for noise from data collection limitations, as well as spatial restrictions. The resulting methodology allows us to infer a network of 19 innexin interactions that govern the formation of gap junctions in *Caenorhabditis elegans*, five of which are already supported by experimental data. As advances in single-cell gene expression profiling increase the accuracy and the coverage of the data, the developed framework will allow researchers to systematically infer experimentally testable connection rules, offering mechanistic predictions for synapse and gap junction formation.

networks | connectome | neuroscience | *C. elegans*

There is ample experimental evidence that the connectome, capturing the neuron-level wiring of a brain, is at least partially genetically encoded. Indeed, while neurons are clustered into broad classes based on their morphology and function, these observed differences between cells are known to be rooted in the differential expression patterns of their genes and proteins (1–10). Consequently, perturbations that alter the genetic identity of individual neurons can induce significant changes in wiring (11, 12). Furthermore, developmental neuroscience has unveiled multiple genetic factors contributing to the formation of neuronal circuits. For example, the connectomes of *Caenorhabditis elegans* and higher organisms rely on a combination of body and wiring localization (13–18), and cell–cell recognition specificity, for both synaptic (19) and gap junction (GJ) connections (11, 20, 21). In the mouse retina, proteins, like connexin-36, play a known role in coupling rods and cones through GJs (22), and, in *D. melanogaster*, neurons expressing the same olfactory receptor converge onto the same set of projection neurons (23). While these studies offer strong experimental support for the genetic roots of neuronal wiring, we continue to lack a general framework to identify the genetic mechanisms that determine the presence or the absence of specific neuronal connections (12, 21, 24).

These advances have prompted the development of statistical approaches designed to identify genes involved in neuronal connectivity. At coarser spatial scales, where collections of spatially proximal neurons are profiled together, data availability has led to the development of correlative and predictive approaches that connect regional gene expression and connectivity in the mouse brain (25, 26). At the neuronal scale, Kaufman et al. (27) demonstrated a correlation between gene expression and neuronal connectivity, and Varadan et al. (28) identified a genetic rule for chemical synapses through an entropy mini-

mization approach. Despite these important advances, existing frameworks fail to incorporate spatial constraints for synapse formation. Indeed, past work in mice, macaque, and *C. elegans* suggests that connection probability decays with spatial distance between soma (17, 29). Strictly speaking, synapses can only exist between neurons in physical contact along their surface. This limitation was recognized by Baruch et al. (30) in their inference of genetic rules, estimating neuronal contact information from neuronal connectivity itself. Here we can take advantage of recent high-resolution efforts to map a neuronal "contactome" in *C. elegans*, that also offer an accurate consideration of spatial and contact information (31). Notwithstanding these promising advances, progress toward unveiling the genetic rules of synapse formation is remarkably slow compared to the tremendous experimental progress focusing on mapping the connectome and the gene expression patterns of individual neurons (32–34).

The gap between experimental and computational progress raises a fundamental question: Is it computationally feasible to infer the genetic rules that govern synapse formation from the available experimental data? For instance, in *C. elegans*, we wish to describe the genetic rules that govern the wiring of neurons of a relatively sparse connectome of $N \approx 300$ neurons (32) using as input the combinatorial expression patterns of $m \approx 20,000$ genes (34). Even if we reduce the genetic complexity to the binary expression of individual genes, m genes can encode a very large number ($N = 2^m$) of neuronal identities. Hence, as we try to infer the list of genes whose expression pattern can encode the observed connectome, we are faced with a heavily

---

Significance

A fundamental question of neuroscience is how the brain wires itself. Here, we propose a modeling framework that explains how cellular connectivity emerges from neuronal identity, allowing us to offer experimentally falsifiable predictions on the genetic encoding of the connectome. The rapid advances in brain science require quantitative frameworks to integrate genetic and connectome information. The proposed model responds to this need, helping us unveil the genetically driven mechanisms that govern the formation of individual links in the brain.

---

[1]To whom correspondence may be addressed. Email: a.barabasi@northeastern.edu.

underdetermined problem: In *C. elegans*, the combinatorial expression of $m = \log_2(N) < 9$ genes is sufficient to fully describe the observed connectome. Although humans have $N \approx$ 86 billion neurons (35), and $m \approx 20{,}000$ genes, the number of neurons is dwarfed by the combinatorial gene expression space of size 2^m, where the expression pattern of m genes determines whether two neurons can synapse. Indeed, if only the binary expression of three genes contributes to synapse formation in each neuron, they allow for $1/6 \times m^3 = 1.3 \times 10^{12}$ combinations, an order of magnitude larger than the number of neurons in a human brain, leading again to serious overfitting. We are therefore faced with an astronomical search space, and the challenge to extract meaningful genetic rules in a heavily ill-conditioned problem of finding them from inherently limited experimental data.

To overcome these difficulties, here we develop a theoretical framework to systematically infer the genetic rules that contribute to the formation and maintenance of synapses and GJs between neurons in contact. We show that these genetic rules can be systematically extracted from three datasets: 1) a comprehensive map of the connectome, 2) a protein expression atlas of the individual neurons, and 3) a list of neurons in physical contact. Finally, we apply our modeling framework to the roundworm *C. elegans*. We do so because the *C. elegans* connectome is believed to be largely identical across individuals (33, 36, 37), and hence predetermined by the genetic markers that label each neuron (5, 20). Yet, the genetic mechanisms that determine which neurons can synapse with each other remain largely unknown even in this simple and well-studied organism (21). We show that we can overcome overfitting by restricting our analysis to genes known to be involved in GJ formation, and developing a spatial connectome model (SCM) to properly account for physical restrictions for wiring. We demonstrate the utility of the proposed modeling framework by predicting 19 interactions between innexin proteins responsible for GJ formation, finding that 5 of them are supported by previous experimental data.

The Connectome Model

We begin with two hypotheses, the first being that each gene can be in two possible states, expressed (one) or not (zero), whose combination defines the genetic barcode for each neuron. As we will discuss later, this hypothesis can be relaxed, but it simplifies the introduction of the connectome model (CM). The second hypothesis states that synapse formation is governed by some (unknown) biological mechanism linked to the gene expression patterns of each pair of neurons (neuronal barcodes). We describe each such mechanism as an operator O, which inspects the barcodes of two neurons and decides to facilitate (or block) the formation of synapses or GJs between them (38).

Consider a hypothetical connectome consisting of seven neurons, A to G, whose connections are uniquely determined by the expression patterns of three genes (Fig. 1*A*). The CM consists of a set of rules that encode the possibility of synapses between genetically encoded sets of neurons (38). As proposed in previous work, a rule could be an abstract operator O_1 that recognizes the complete genetic profile of neurons C and G, designating C as a source and G as a destination neuron, and establishing synapses between them (Fig. 1*B*). The connections that result can be either undirected, as in the case of GJs, or directed, like synapses (*SI Appendix, Chemical Synapses*). However, a less specific operator (O_2 or O_3), that detects only a subset of the genes, ignoring the expression state of the genes marked by X, can generate multiple links between two sets of neurons, like the complete biclique of eight links in Fig. 1*D*. Fig. 1 summarizes a key prediction of the CM: Each biological mechanism that relies on gene expression to initiate synapse formation will generate an imprint in the connectome in the form
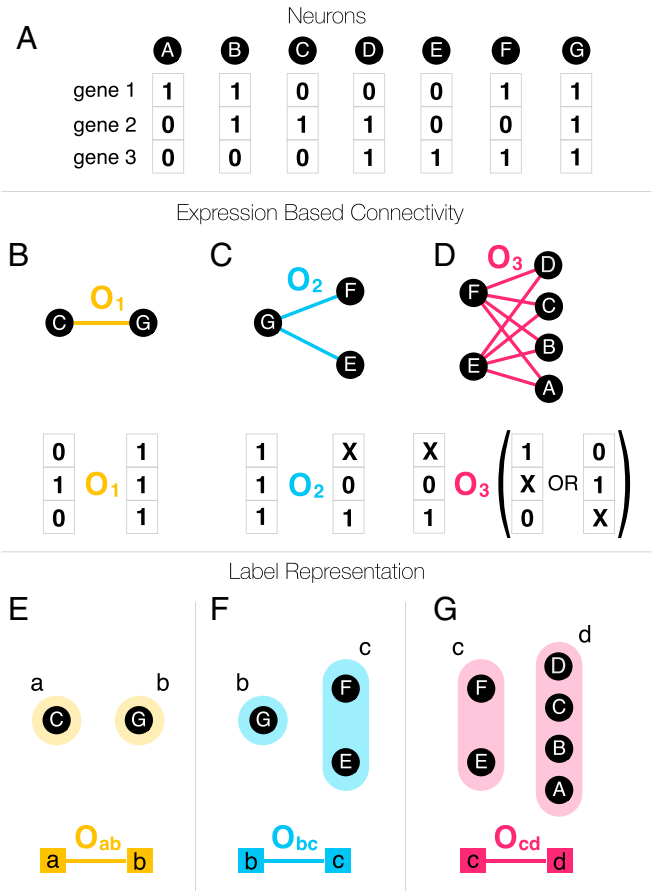

Fig. 1. Genetic labels. (*A*) The terminal expression profile of seven neurons (black nodes), involving three genes, expressed (one) or unexpressed (zero). (*B*) The formation of links (chemical synapses, gap junctions) are governed by the expression profiles of the neurons, through biological mechanisms that have previously been abstracted as operators, O_i (38). In the simplest case, an operator recognizes the full expression pattern of neurons C and G and connects them. (*C*) A single rule or operator can generate multiple links, if the operator detects the expression of some genes and ignores others. Here, X marks the gene ignored by the operator, whether it is expressed or not. (*D*) More complex operators that have multiple Xs in them can facilitate a large number of links. (*E*) In the formalism proposed here, we assign two labels to each operator, one to the source neurons (left) and another to the destination neurons (right). The labels allow us to represent operator O_1 as a link connecting the neurons with the right labels. (*F*) Even if the same label is assigned to multiple neurons, the operator O_2 remains a simple link between the two labels. (*G*) While the operator O_3 might appear complicated in terms of the original gene expression data, it has a simple structure in the label representation.

of a unique network motif, known as a *noninduced biclique* in graph theory (39) (see also *SI Appendix*, Fig. S1), where neurons of the source set can be connected to neurons of the destination set. Ref. 39 validated this prediction by showing an excess of specific large biclique motifs in the *C. elegans* connectome. The challenge, which we address here, is how to reverse engineer the genetic rules from the observed network patterns, given that even a modest number of genetic rules can lead to a tremendous number of network motifs. Furthermore, the genetic rules can be rather complex when expressed in terms of operators connecting gene expression patterns (Fig. 1*D*), rooted in the nonlinear representation of combinatorial expression data. In order to make the description mathematically tractable, we introduce genetic labels, allowing us to capture multiple genetic operators within a single network-based framework. For instance, we can rewrite O_1 as the operator O_{ab}, where we assign all

participating source neurons the label "a" (Fig 1E) and assign all destination neurons the label "b" (Fig. 1E). A biological rule governing neural connections between the source and destination neurons can be represented by the link $a-b$ between the two labels.

In this label-based representation, the operators have a simple form (Fig. 1 E–G), and the complexity of a rule is incorporated in how genes define the labels. Although some labels can represent complex gene expression patterns (e.g., Fig. 1D), others can be very simple. For example, electrical synapses or GJs are intercellular channels formed by two matching hemichannels consisting of a subset of 25 innexin proteins (40). In order to maintain a GJ, the innexins forming the hemichannels must be expressed on the surface of neurons in contact. In our formalism, the simplest rule, O_{ab}, is then a link between two innexins "a" and "b" expressed on two neurons forming a GJ. In other words, we assign label "a" (or "b") to each neuron if it expresses innexin "a" (or "b"). In general, GJs can be also heteromeric, requiring a label that corresponds to the simultaneous expression of two (or more) innexins.

The labeling of each neuron is summarized in the expression matrix (X), where $X_{ia} = 1$ if neuron i's expression pattern is consistent with label "a," and zero otherwise (Fig. 2A). The rule matrix O summarizes the individual operators as links connecting the labels (Fig. 2B). If two neurons in contact express labels that are connected in O, then there is a nonzero chance of establishing a synapse between these neurons. This representation defines mathematically the CM, that links the brain's connectome (B) to the expression patterns of the individual neurons X, through the rule matrix O,

$$B = XOX^T. \tag{1}$$

The CM (Eq. **1**) is our first key result, formally linking the connectome (B), the expression patterns of the individual neurons (X), and the biological mechanisms (O) that govern synapse/GJ formation in the brain. Eq. **1** is valid for weighted label expression data as well, where the weights capture the probability that a given neuron agrees with a given label.

In practice, not all of the genetically allowed connections can be observed, due to experimental limitations, developmental and spatial constraints, and neural plasticity. In our formalism, this implies that O is a stochastic operator with O_{ab} not necessar-

ily being 1 (Fig. 3). For instance, fruit fly inx-2 homomeric GJs form only between 40% of the neighboring cell pairs (41), leading to an apparent stochasticity in GJ formation, corresponding to $O_{aa} = 0.4$. In the absence of such stochastic effects, O_{aa} predicts a complete subgraph of all a label neurons. With stochasticity, instead of a fully connected subgraph, we expect a community of nodes connected to each other with density $O_{aa} = 0.4$ (Fig. 3E). In other words, O is a weighted matrix, where the weights are the probabilities that neurons carrying labels "a" and "b" will link to each other.

Taken together, as the CM (Eq. **1**) establishes a direct connection between the expression profiles of the individual neurons (X) and the connectome (B) through genetic rules (O), it allows us to address several key problems in brain science, listed in the order of increasing technical difficulty: 1) Map out the connectome: Predict the connectome (B) from gene expression (X) and the genetic rules (O). 2) Unveil the genetic rules: Predict the genetic rules (O) behind the connectome from known X and B. 3) Predict expression patterns: Find the gene expression of neurons (X) from the genetic rules (O) and the wiring of the connectome (B).

Problem 1 is readily solved by Eq. **1**, assuming that we know (some of) the biological mechanisms behind the rules in O. As we currently lack these rules, in this paper, we focus on the pressing issue of solving Problem 2. This choice is motivated by the fact that, in *C. elegans*, we have a comprehensive map of its neural system's adjacency matrix (B) and extensive (yet somewhat noisy and incomplete) information on the gene expression patterns of individual neurons (X), potentially allowing us to determine the biological mechanisms encoded in O.

Solving the Connectome Model. Given the connectome B and the labels X, our goal is to identify the operator O that collects the biological rules that govern link formation (Problem 2). To illustrate the procedure, we use the three rules introduced in Fig. 1 to generate the brain connectome B (Fig. 2C), according to the label expression X (Fig. 2A). In the occasion of multiple rules contributing to the same link in the connectome, B is a weighted matrix, with the weight of each link corresponding to the number of rules involved. Generally, just by looking at two connected neurons, it appears impossible to reverse the problem and infer the genetic rule responsible for each connection (Fig. 2A, neurons C and G). Indeed, the rule could connect label "a" to label
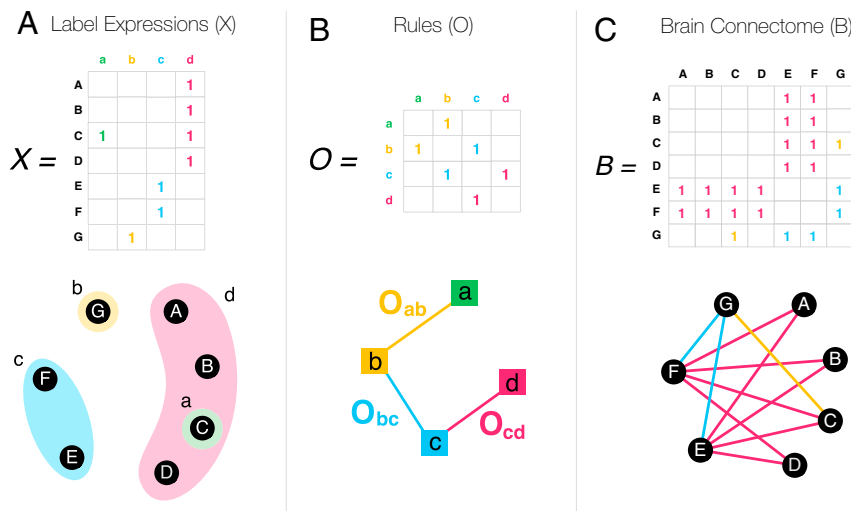

Fig. 2. The CM. (A) The expression pattern of the neurons A to G are summarized in the label expression matrix X. (B) The operators connecting the labels can be summarized in the organizing rule matrix O. (C) In the CM, the brain connectome (B) emerges from O and X through the CM Eq. **1**. Each time two labels are connected in O, the corresponding neurons in X can form synapses. Only nonzero elements are shown in the matrices.
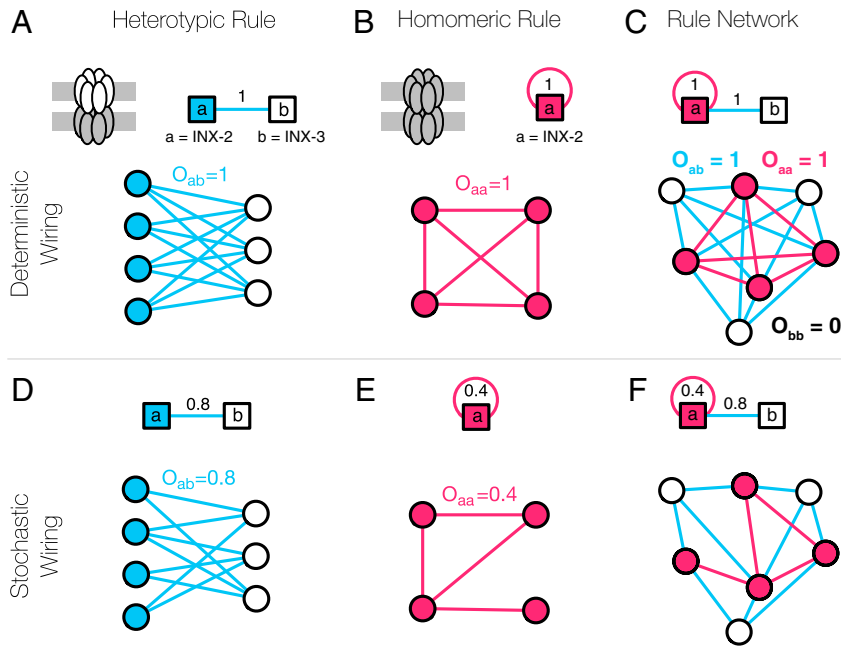
Fig. 3. GJs in the CM. GJs are formed by interacting hemichannels comprising innexin proteins. In the simplest case, a hemichannel is made of a single innexin, meaning that the expressed innexins can directly serve as labels. (*A*) Two *Drosophila* innexin proteins, inx-2 and inx-3, have been found to form (heterotypic) GJs, resulting in multiple potential neural connections (41). (*B*) There is evidence that inx-2 can form homomeric GJs, establishing connections between the neurons expressing inx-2, represented by the self-loop in the figure. (*C*) Altogether, the two rules (*A* and *B*) can be integrated into a rule network that serves as a genetic template for the GJ connectome. (*D*) The formalism behind the CM allows for stochastic rules, that is, a weight of 0.8 indicates that 80% of the potential neural connections are present in the brain. This stochasticity can arise from multiple factors, including noisy or incomplete expression and connectome data, spatial effects, biological constraints, and true stochasticity of neuronal wiring. (*E*) According to oocyte experiments (51), the homomeric innexin rule of *Drosophila* inx-2 has a weight of 0.4, as only 40% of the possible links are observed. (*F*) Even in the presence of apparent or true stochasticity, we can capture the GJ connectome using only a few (weighted) innexin rules.

"b," but could also connect label "a" to label "d." Even if we had simultaneous access to the complete list of neural connections (B) and full genetic labels (X), inferring the rules responsible for link formation (O) is mathematically ill conditioned, with infinitely many solutions of the form

$$\tilde{O} = X^+ B X^{+T} + W - X^+ X W X^T X^{+T}, \qquad [2]$$

where W is an arbitrary matrix and X^+ stands for the Moore–Penrose pseudoinverse of X, which has the property $XX^+X = X$ (42). We have a unique solution only when $X^+ = X^{-1}$, meaning that the neurons have linearly independent label expression patterns, which is not expected to be the case in the brain. Otherwise, even if there is no noise in the input data, we do not expect to find an exact solution, and $\tilde{O}$ comes with a least-square residual error $r^2 = \|B - X\tilde{O}X^T\|^2 > 0$. In practice, the situation is even more difficult because B and X have multiple unknown errors (both false negatives and false positives). To make progress, we invoke the parsimony principle, searching for the model that accounts for the available data with the fewest rules in O. A convenient way to mathematically formalize this is to minimize the objective function with a regularization parameter $\alpha \geq 0$,

$$r^2 + \alpha\|O\|^2, \qquad [3]$$

where $\|O\|^2 \equiv \sum_{ij} O_{ij}^2$ is the square of the Frobenius norm. When O consists of only zeros and ones, a minimal Frobenius norm corresponds to the fewest rules or the fewest ones in the O matrix. As an alternative implementation of the parsimony principle, we could also select the sum of the absolute values in O as the norm, related to compressed sensing, also known as LASSO (least absolute shrinkage and selection operator) (43). Here, we proceed with the Frobenius norm in order to maintain

the analytical tractability of the problem, and to be able to assess the significance of the obtained rules. With this, we can find the optimal O, relying on the results on ridge regression (Tikhonov regularization) (44), discussed in *Methods*.

The SCM

The CM assumes that each neuronal connection allowed by the genetic profile of the neurons will form with a probability dictated by genetics only. Yet, for a synapse or GJ to form, the neurons must also be in physical contact (Fig. 4*A*). If we ignore these spatial constraints, each missing link between remote neurons is taken as evidence against the rule, including links allowed by the genetics that do not have the opportunity to form as the neurons do not come in contact (Fig. 4*B*). Therefore, to increase the accuracy of the model's predictions, we must restrict our analysis to pairs of neurons that do touch each other. This information is encoded by the contact matrix C, telling us which neuron pairs are in physical contact. In *C. elegans*, the anterior brain contactome (C) has been mapped experimentally (45), prompting us to restrict our analyses to the anterior 185 neurons detailed in ref. 31 and available at https://wormwiring.org. Altogether, 5,592 neuron pairs are in physical contact, representing ∼33% of all pairs, out of which only 601 form GJs.

It is tempting to incorporate spatial constraints into our matrix representation (Eq. **1**) by ignoring each matrix element in B that is absent in the contact matrix C (Fig. 4*C*). If we do so, the obtained truncated matrix has nonexisting entries (Fig. 4*C*), and we cannot apply standard matrix operations to it. The naïve choice of treating each missing link as a zero in the connectome matrix leads to incorrect rules, as illustrated in Fig. 4*D*. To address this problem, we represent the connectome B as an edge list rather than a matrix. In other words, we rearrange the connectome matrix B (by any, i.e., lexicographic order) into the
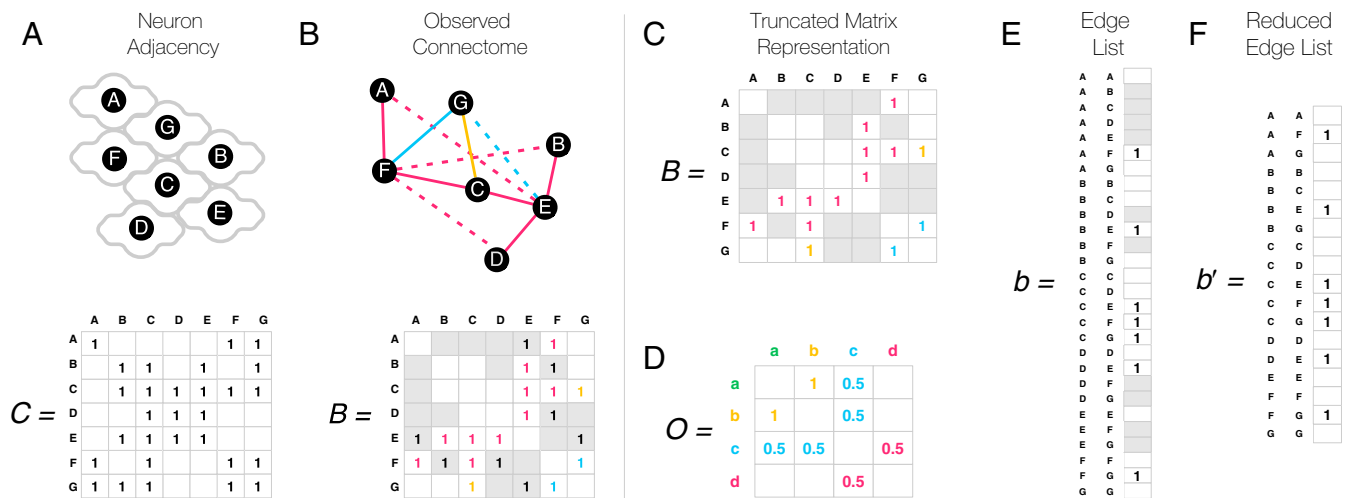
Fig. 4. The SCM. (*A*) Neurons can only synapse if they are in physical contact. We schematically indicate physical contacts via touching neuron contours in the figure, and contacting neuron pairs are marked by a one in the matrix *C*. Note that neurons can be in physical contact with themselves and even form synapses. (*B*) Given the lack of physical contact, only a fraction of the genetically allowed synapses are observed. The dashed links in the network, shown as ones in gray cells in the adjacency matrix below, indicate neural connections that are genetically permitted but are not observed because the neurons are not in contact. (*C*) When inferring genetic rules, distant neuron pairs must be ignored in the model (gray cells), as we do not know whether the lack of connection has a genetic origin or is simply due to spatial constraints. We therefore arrive at a truncated matrix representation, which does not obey standard matrix operations, and hence is challenging to work with. (*D*) If we treat all unobserved cells (gray and blank) as zeros, the matrix representation leads to incorrect rules, as it always assumes the lack of genetic compatibility where there may be some. (*E*) The edge list representation offers a linear description that is formally equivalent with the matrix representation. (*F*) Distant pairs of neurons can be removed from the edge list representation, and, as a truncated list is still a list, it allows us to uncover the correct rules based on Eq. **5**.

connectome vector $b = \text{vec}(B)$ (Fig. 4*E*). Similarly, we rearrange the rule matrix *O* into a rule vector $o = \text{vec}(O)$. This allows us to reformulate the bilinear CM in Eq. **1** as a higher-dimensional linear model

$$b = Ko, \qquad [4]$$

where $K = X \otimes X$ is the Kronecker product. This, so far equivalent, linear representation allows us to restrict the space of neural connections to neurons in physical contact, by ignoring the entries in *b* and *K* that do not satisfy physical contact according to the *C* matrix, resulting in a reduced *b'* and *K'* (Fig. 4*F*). We therefore arrive at the truncated connectome model describing the SCM, representing our second key result,

$$b' = K'o. \qquad [5]$$

This equation can be solved using tools similar to the ones we used to study the CM, as discussed in *Methods*. At the end, the obtained rule weights vector $\tilde{o}$ can be rearranged into a matrix format, $\tilde{O}$. If we perform these calculations on the toy model of Fig. 2 *A* and *C* with the indicated spatial constraints, we recover the exact rules in Fig. 2*B*, even though we are using only a fraction of the connectome information, that is, only the links that are between touching neurons. This result suggests that we do not need complete input data on the *C. elegans* connectome and gene expression to make reliable predictions, as we can use Eqs. **5** and **7** to uncover the biological mechanisms *O* governing brain wiring even from partial data. Yet, we need to know the genetic labels, that is, the genetic basis, *X*, in which the organizing rules operate. Next, we show how Eq. **5** helps us unveil the biological mechanism governing GJ formation.

Unveiling the Rules behind GJs

Electrical synapses, or GJs, play an important role in the *C. elegans* nervous system and muscle control (46). There are 25 genes involved in *C. elegans* GJ formation, all of which encode innexin proteins (collectively called innexin genes, even though not all of them are named inx*). We can therefore ignore the expression

patterns of noninnexin genes, limiting overfitting by restricting the genetic space in *X* used in our analysis. Currently, there is published expression data for 18 of the 25 innexin genes in *C. elegans* neurons (45) The innexin expression data we rely on were collected by a single group using a consistent method (45), and we relied on a curated version of the expression data that ensures the best available representation in terms of zeros and ones (5). Nevertheless, the data are expected to be enriched with zeros, resulting both from experimental error and incomplete studies. These omissions lead to inconsistencies: Although every neuron class is known to form GJs, about one-third of the neurons have no reported innexin gene expressed (47, 49). Besides this obvious data incompleteness, the expression data are also limited by experimental difficulties of differentiating between individual neurons within the same neuron class, practically limiting the resolution of the expression data to neuron classes. With these data limitations in mind, as a first step, we consider only the genetic labels linked to the expression patterns of individual innexin genes.

We begin by applying Eq. **7**, using, as input, the innexin gene expression data (*X*) (45), the GJ connectome (*B*) (33), and the neuronal contactome *C* (34, 45), aiming to calculate *O*, describing the genetic rules that govern GJ formation (Fig. 5 and *Methods*). We set the regularization parameter at its optimal value $\alpha = 0.215$ (*Methods* and *SI Appendix*, Fig. S2), but we find that our results are qualitatively similar if we rely on any smaller, nonoptimized $\alpha > 0$ (*SI Appendix*, Fig. S6). The elements of the obtained $\tilde{O}$ matrix represent the probability that neurons expressing those genes form GJs due to this specific genetic rule. Most of the obtained rules have a small, but nonzero, weight (*SI Appendix*, Fig. S3), which is expected due to the chosen Frobenius norm, and also because of weight inflation resulting from false negatives in the expression data. We must therefore differentiate small values from meaningful probabilities. To assess the significance of the results, we developed a method to perform degree-preserving randomization of the connectome (49) without violating the spatial constraints. Indeed, while keeping
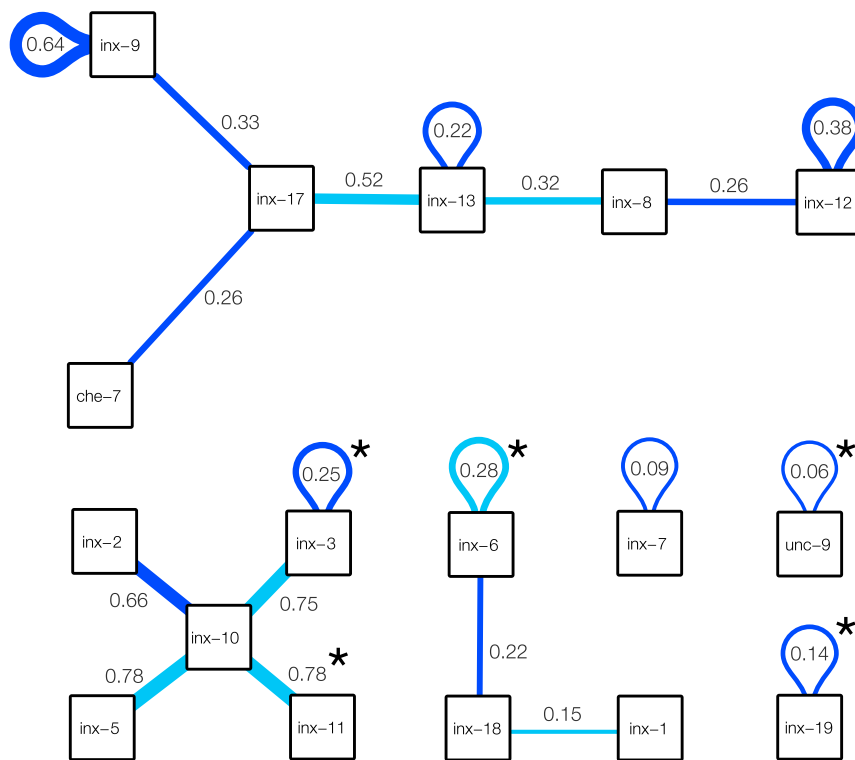
Fig. 5. Predicted innexin rules. Significant innexin rules inferred for *C. elegans* GJs, showing only positive rules with a *z* score of at least 2. Each box corresponds to an innexin protein in *C. elegans*. Dark blue links are found to be significant in both connectome reconstructions (*SI Appendix*, Fig. S4), while light blue links are significant only in the Cook et al. (33) connectome. Link weights estimate the connection probability. For example, the link between inx-2 and inx-10 has weight 0.66, meaning that the neurons expressing these two innexins establish GJs in 66% of the cases. Note that the observed probability of GJs between these neurons might change if multiple rules contribute to them.

the node (neuron) degrees unchanged is a standard requirement of a proper null model (49), we lack methods to perform such randomization without generating interactions between noncontacting pairs of neurons. We therefore developed a maximum entropy approach for network randomization with spatial constraints, using a subgraph randomization protocol (see *Methods*), allowing us to readily determine the *z* score for each predicted rule. The *z* scores can then be used to rank the obtained rules for validation experiments.

With the standard $z > 2$ threshold, we find 19 significant wiring rules, summarized in Fig. 5 (for all *z* scores, see *SI Appendix*, Fig. S3). Five of the 19 rules have been uncovered previously by the experimental literature, including 1) **inx-19–inx-19** ($z = 3.4$) (46), 2) **unc-9–unc-9** ($z = 3.1$) (46), 3) inx-10–inx-11 ($z = 3.0$) (50), 4) **inx-3–inx-3** ($z = 2.8$) (46), and 5) inx-6–inx-6 ($z = 2.5$) (46), where the boldface font indicates that the interaction is significant for two different *C. elegans* connectome reconstructions (*SI Appendix*, Fig. S4). Given that no further single innexin interactions were found in literature, observing all five experimentally supported interactions out of a set of 19 predictions appears to be highly significant ($p \approx 10^{-5}$). However, this observation is tempered by the facts that the experiments relied on multiple methods: the inx-19–inx-19 interaction was confirmed by electrically coupling *Xenopus* oocytes (51), while inx-6–inx-6 channels have been confirmed by EM reconstruction (52). The remaining interaction rules are uncovered by the model: 6) **inx-12–inx-12** ($z = 5.6$), 7) **inx-9–inx-9** ($z = 5.0$), 8) inx-3–inx-10 ($z = 3.4$), 9) inx-5–inx-10 ($z = 3.0$), 10) inx-8–inx-13 ($z = 2.8$), 11) **che-7–inx-17** ($z = 2.8$), 12) **inx-8–inx-12** ($z = 2.6$), 13) **inx-9–inx-17** ($z = 2.5$), 14) **inx-6–inx-18** ($z = 2.4$), 15) **inx-7–inx-7** ($z = 2.4$), 16) **inx-13–inx-13** ($z = 2.4$), 17) inx-13–inx-17 ($z = 2.4$), 18) **inx-2–inx-10** ($z = 2.1$), and 19) inx-1–inx-18 ($z = 2.0$), where

boldface again indicates that the interaction is confirmed in both reconstructions (*SI Appendix*, Fig. S4).

The obtained interactions offer ground for direct falsifiable experimental confirmation, for example, by expressing one of each innexins in *Xenopus* oocytes and checking for electric coupling. In addition, it is possible to introduce genetic interventions that, according to our model, are expected to lead to rewiring in the *C. elegans* system. The developed framework allows us to predict the nature of this rewiring: For example, if a connection between two neurons is due to a single rule, then losing the participating genetic label on either side leads to a loss of interaction. For instance, our inference predicts that the AINR–ASGL and AINL–ASGR GJs, present in both *C. elegans* connectome reconstructions, are coded solely by the che-7–inx-17 rule, an interaction found to be significant according to inference on both reconstructions (*SI Appendix*, Fig. S4). Therefore, knocking down any of these genes in the neurons, or pharmacologically preventing the interaction, is expected to result in the loss of these two GJs. Note that these predictions are sensitive to the noise in the input data and the choice of the significance threshold, particularly since all single-rule GJs originate from low-strength interactions.

Discussion

Motivated by the need to infer the genetic rules that govern the wiring diagram of the connectome, here we have introduced a computational framework that relates the genetic expression profiles of the individual neurons to the connectome. Although the connectome and, especially, the neuron gene expression profiles remain heavily incomplete and prone to noise, our results indicate that their joint coverage is sufficient to infer some of the conjectured interactions that govern GJ formation in the

C. elegans nervous system. To achieve this, we established a connection between the gene expression patterns of single neurons and the connectome, through the CM (Eq. **1**). As synapses can only form between neurons that are in physical contact, we incorporated spatial constraints in our framework, resulting in the SCM (Eq. **5**). The model allowed us to identify 19 significant innexin rules behind GJs. As the availability of high-quality input data increases, the SCM can be extended to capture chemical synapse formation, which follows the same constraints as GJs (53), helping to illustrate the versatility of the developed modeling framework (*SI Appendix, Chemical Synapses*).

Although we utilized the multimodal profiling of *C. elegans* to validate specific predictions, the SCM formalism is developed to meet future needs, in expectation of new connectomes and detailed genetic profiling methods. Indeed, working with larger connectomes highlights the importance of incorporating constraints, as, in large connectomes, an overwhelming fraction of neuron pairs are not in physical contact. The presented framework offers guidance for future experiments: To apply SCM to these systems requires a matched connectome, contactome, and transcriptome, meaning that, for each cell, we need to know its connections, its physical contacts, and its gene expression. Partial neuronal transcriptomes and connectomes have been published recently for fly (54–56) and zebrafish (57, 58). However, connectivity and gene expression were not profiled jointly; thus these datasets cannot offer cellular-level predictions. In an alternate application, future work could utilize the CM to infer genetic correlates of projectomic rules, where the B matrix can be a projectome, such as between neuronal areas, and X remains a label-transformed transcriptome, while O represents genetic compatibility rules that promote projections from one region to another. This application may require us to alter the subgraph randomization procedure to account for a weighted connectome, which could be achieved by redefining the maximum entropy constraints (59, 60).

The SCM, together with the inferred innexin rules, allows us to predict potential changes in neural wiring if gene expression is altered via knockout experiments or silencing. Yet, a knockout experiment of an innexin is only informative if the mutant is viable. The individual loss of several innexins (including inx-3, inx-12, inx-13, inx-14, and inx-22) is known to be lethal (46), limiting knockout experiments to nonessential innexins, unless, maybe, the experiments can be limited to specific neurons only. Temperature-sensitive alleles provide an alternative way to experimentally modulate the expression of essential innexins, keeping the innexins functional during development, and disabling the corresponding GJs at restrictive temperatures (61, 62). Another possibility would be an exercise in edgetics, that is, disrupting specific protein–protein interactions using drugs targeting innexins (63), and detecting the resulting change in the connectome. Our model could also be used to predict how the brain is rewired in the food-deprived, dormant state of the *C. elegans* known as the dauer stage. Functional studies indicate a substantial remodeling of behavior which anticipates a substantial rewiring of the GJ connectome, with profound impact on synaptic partner choices. As a prerequisite, dauer-stage neuron gene expression data have been made available recently (47).

Finally, as the SCM establishes connections between brain connectivity and genetics, we can assess whether neurons are primarily connected based on genetic similarity (*SI Appendix, Spectral Interpretation of the Wiring Rules*). The diagonalization of the rule matrix (O) leads to a minimal set of abstract rules, given by the eigenvalues. If all eigenvalues are nonnegative, that indicates that neurons will form synapses with other neurons of similar expression profiles. We find, however, at least four negative eigenvalues, supporting a complex genetic organization (*SI Appendix*, Fig. S5), with a strong presence of genetic heterophily, indicating that GJ formation relies strongly on genetic complementarity besides similarity.

Methods

Ridge Regression. The optimization problem (Eq. **3**) can be solved analytically as (44)

$$\tilde{O} = X^+(\alpha)BX^{+T}(\alpha), \qquad [6]$$

where $X^+(\alpha) = (X^T X + \alpha I)^{-1} X^T$. In the $\alpha \to 0$ limit, the solution is $\tilde{O} = X^+ B X^{+T}$, yielding the best residual error (r^2) at the expense of the simplicity of O, prone to overfitting in the presence of errors. This limit is also sensitive to changes in B; therefore, $\alpha \to 0$ is only appropriate when the input data are exact. In contrast, $\alpha \to \infty$ leads to the estimate $\tilde{O} \propto X^T BX$, coinciding with the naïve assumption discussed in ref. 28, yielding a poor r^2, being prone to underfitting. Here we find the optimal α, following the suggestion by Wahba and coworkers (64), proven to be optimal in a generalized cross-validation scenario, corresponding to α that minimizes r^2/τ^2, where $\tau = \text{Tr}(I - KK^+(\alpha))$, and $K = X \otimes X$ is calculated using the Kronecker product. Eq. **5** can be solved similarly, leading to

$$\tilde{o} = K'^+(\alpha)b', \qquad [7]$$

with $K'^+(\alpha) = (K'^T K' + \alpha I)^{-1} K'^T$, at the optimal α, minimizing r^2/τ^2, with $\tau = \text{Tr}\left(I - K'K'^+(\alpha)\right)$ (*SI Appendix*, Fig. S2).

Subgraph Randomization. We start with a graph G_0 and a subgraph G_1, and we aim to sample, uniformly, the space of subgraphs of G_0 with (approximately) the same subgraph degree sequence as given in G_1. This represents a constrained version of the traditional degree-preserved randomization, where G_0 is a complete graph (65), as all interactions that are not in G_0 appear as hard constraints and are excluded from the randomized networks. Here, G_0 represents the list of neurons in contact that could, in principle, establish a GJ, and we randomize the network of existing synapses without violating the known neuronal contact structure (C). We use a maximum entropy approach, maximizing the entropy of the random network ensemble defined as $S = -\sum_G P(G) \ln P(G)$. The average subgraph degree of each node in G_1 is $\langle k_i \rangle = \sum_G P(G)k_i(G)$, which we keep fixed at the original value, k_i. The probability of a given graph instance is $P(G) = e^{-H(G)}/Z$, where $H = \sum_i \beta_i k_i(G)$, and the probability of having a link between nodes i and j is expressed as $p_{ij} = 1/1 + \alpha_i \alpha_j$, where $\alpha_i = e^{-\beta_i}$. The average subgraph degree of a node is then given by $\langle k_i \rangle = \sum_{j,(i,j) \in G_0} \frac{1}{1+\alpha_i \alpha_j}$, and the optimal α can be found iteratively, with the update rule

$$\alpha_i' = \frac{1}{k_i} \sum_{j,(i,j) \in G_0} \frac{1}{\alpha_j + 1/\alpha_i}, \qquad [8]$$

starting from the initial condition $\alpha_i^{(0)} \equiv 1$ leading to $\alpha_i^{(1)} = K_i/2k_i$, where K_i is the full node degree in G_0. We perform a hundred iterations to estimate the optimal α, allowing us to calculate the mean and the variance of the randomized matrix ensemble. Due to the linearity of the SCM solution, these yield a z score for each inferred wiring rule (through the first and second moments), without the need of explicitly generating random samples from the ensemble.

1. A. Paul *et al.*, Transcriptional architecture of synaptic communication delineates gabaergic neuron identity. *Cell* **171**, 522–539 (2017).
2. H. S. Seung, U. Sümbül, Neuronal cell types and connectivity: Lessons from the retina. *Neuron* **83**, 1262–1272 (2014).
3. B. Tasic *et al.*, Adult mouse cortical cell taxonomy revealed by single cell transcriptomics. *Nat. Neurosci.* **19**, 335–346 (2016).
4. A. Zeisel *et al.*, Cell types in the mouse cortex and hippocampus revealed by single-cell RNA-seq. *Science* **347**, 1138–1142 (2015).

5. O. Hobert, L. Glenwinkel, J. White, Revisiting neuronal cell type classification in *Caenorhabditis elegans. Curr. Biol.* **26**, R1197–R1203 (2016).

6. G. Fishell, A. Kepecs, Interneuron types as attractors and controllers. *Annu. Rev. Neurosci.* **43**, 1–30 (2019).

7. M. B. Reilly, C. Cros, E. Varol, E. Yemini, O. Hobert, Unique homeobox codes delineate all the neuron classes of *C. elegans. Nature* **584**, 595–601 (2020).

8. L. Lim, D. Mi, A. Llorca, O. Marín, Development and functional diversification of cortical interneurons. *Neuron* **100**, 294–313 (2018).

9. D. F. English *et al.*, Pyramidal cell-interneuron circuit architecture and dynamics in hippocampal networks. *Neuron* **96**, 505–520 (2017).

10. L. Warren *et al.*, Highly efficient reprogramming to pluripotency and directed differentiation of human cells with synthetic modified mRNA. *Cell Stem Cell* **7**, 618–630 (2010).

11. I. Rabinowitch, W. R. Schafer, Engineering new synaptic connections in the *C. elegans* connectome. *Worm* **4**, e992668 (2015).

12. R. A. Carrillo *et al.*, Control of synaptic connectivity by a network of *Drosophila* IgSF cell surface proteins. *Cell* **163**, 1770–1782 (2015).

13. W. Y. Timothy, J. C. Hao, W. Lim, M. Tessier-Lavigne, C. I. Bargmann, Shared receptors in axon guidance: SAX-3/Robo signals via UNC-34/enabled and a netrin-independent UNC-40/DCC function. *Nat. Neurosci.* **5**, 1147–1154 (2002).

14. Y.-s. Lim, W. G. Wadsworth, Identification of domains of netrin UNC-6 that mediate attractive and repulsive guidance and responses from cells and growth cones. *J. Neurosci.* **22**, 7080–7087 (2002).

15. E. M. Hedgecock, J. G. Culotti, D. H. Hall, The UNC-5, UNC-6, and UNC-40 genes guide circumferential migrations of pioneer axons and mesodermal cells on the epidermis in *C. elegans. Neuron* **4**, 61–85 (1990).

16. C. E. Adler, R. D. Fetter, C. I. Bargmann, UNC-6/netrin induces neuronal asymmetry and defines the site of axon formation. *Nat. Neurosci.* **9**, 511–518 (2006).

17. M. Ercsey-Ravasz *et al.*, A predictive network model of cerebral cortical connectivity based on a distance rule. *Neuron* **80**, 184–197 (2013).

18. Y. Han *et al.*, The logic of single-cell projections from visual cortex. *Nature* **556**, 51–56 (2018).

19. K. Shen, R. D. Fetter, C. I. Bargmann, Synaptic specificity is generated by the synaptic guidepost protein SYG-2 and its receptor, SYG-1. *Cell* **116**, 869–881 (2004).

20. G. Marcus, A. Marblestone, T. Dean, The atoms of neural computation. *Science* **346**, 551–552 (2014).

21. T. C. Südhof, Synaptic neurexin complexes: A molecular code for the logic of neural circuits. *Cell* **171**, 745–769 (2017).

22. G. Söhl, S. Maxeiner, K. Willecke, Expression and functions of neuronal gap junctions. *Nat. Rev. Neurosci.* **6**, 191–200 (2005).

23. W. Hong, L. Luo, Genetic control of wiring specificity in the fly olfactory system. *Genetics* **196**, 17–29 (2014).

24. A. T. DePew, M. A. Aimino, T. J. Mosca, The tenets of teneurin: Conserved mechanisms regulate diverse developmental processes in the *Drosophila* nervous system. *Front. Neurosci.* **13**, 27 (2019).

25. A. Arnatkeviciute, B. D. Fulcher, A. Fornito, Uncovering the transcriptional signatures of hub connectivity in neural networks. *Front. Neural Circ.* **13**, 47 (2019).

26. A. Fakhry, S. Ji, High-resolution prediction of mouse brain connectivity using gene expression patterns. *Methods* **73**, 71–78 (2015).

27. A. Kaufman, G. Dror, I. Meilijson, E. Ruppin, Gene expression of *Caenorhabditis elegans* neurons carries information on their synaptic connectivity. *PLoS Comput. Biol.* **2**, e167 (2006).

28. V. Varadan, D. M. Miller III, D. Anastassiou, Computational inference of the molecular logic for synaptic connectivity in *C. elegans. Bioinformatics* **22**, e497–e506 (2006).

29. A. Arnatkeviciute, B. D. Fulcher, R. Pocock, A. Fornito, Hub connectivity, neuronal diversity, and gene expression in the *Caenorhabditis elegans* connectome. *PLoS Comput. Biol.* **14**, e1005989 (2018).

30. L. Baruch, S. Itzkovitz, M. Golan-Mashiach, E. Shapiro, E. Segal, Using expression profiles of *Caenorhabditis elegans* neurons to identify genes that mediate synaptic connectivity. *PLoS Comput. Biol.* **4**, e1000120 (2008).

31. C. A. Brittin, S. J. Cook, D. H. Hall, S. W. Emmons, N. Cohen, Volumetric reconstruction of main *Caenorhabditis elegans* neuropil at two different time points. bioRxiv:485771 (4 December 2018).

32. L. R. Varshney, B. L. Chen, E. Paniagua, D. H. Hall, D. B. Chklovskii, Structural properties of the *Caenorhabditis elegans* neuronal network. *PLoS Comput. Biol.* **7**, e1001066 (2011).

33. S. J. Cook *et al.*, Whole-animal connectomes of both *Caenorhabditis elegans* sexes. *Nature* **571**, 63–71 (2019).

34. T. W. Harris *et al.*, Wormbase: A comprehensive resource for nematode research. *Nucleic Acids Res.* **38**, D463–D467 (2010).

35. F. A. Azevedo *et al.*, Equal numbers of neuronal and nonneuronal cells make the human brain an isometrically scaled-up primate brain. *J. Comp. Neurol.* **513**, 532–541 (2009).

36. T. A. Jarrell *et al.*, The connectome of a decision-making neural network. *Science* **337**, 437–444 (2012).

37. D. S. Walker, Y. L. Chew, W. R. Schafer, "Genetics of behavior in *C. elegans*" in *The Oxford Handbook of Invertebrate Neurobiology*, J. H. Byrne, Ed. (Oxford University Press, 2017).

38. D. L. Barabási, A. L. Barabási, A genetic model of the connectome. *Neuron* **105**, 435–445 (2020).

39. B. Zelinka, On a problem of E. Prisner concerning the biclique operator. *Math. Bohem.* **127**, 371–373 (2002).

40. D. H. Hall, Gap junctions in *C. elegans*: Their roles in behavior and development. *Dev. Neurobiol.* **77**, 587–596 (2017).

41. L. A. Stebbings, M. G. Todman, P. Phelan, J. P. Bacon, J. A. Davies, Two *Drosophila* innexins are expressed in overlapping domains and cooperate to form gap-junction channels. *Mol. Biol. Cell* **11**, 2459–2470 (2000).

42. M. James, The generalised inverse. *Math. Gaz.* **62**, 109–114 (1978).

43. R. Tibshirani, Regression shrinkage and selection via the lasso. *J. Roy. Stat. Soc. B* **58**, 267–288 (1996).

44. A. E. Hoerl, R. W. Kennard, Ridge regression: Biased estimation for nonorthogonal problems. *Technometrics* **12**, 55–67 (1970).

45. Z. F. Altun, B. Chen, Z. W. Wang, D. H. Hall, High resolution map of *Caenorhabditis elegans* gap junction proteins. *Dev. Dynam.* **238**, 1936–1950 (2009).

46. K. Simonsen, D. Moerman, C. C. Naus, Gap junctions in *C. elegans. Front. Physiol.* **5**, 40 (2014).

47. A. Bhattacharya, U. Aghayeva, E. G. Berghoff, O. Hobert, Plasticity of the electrical connectome of *C. elegans. Cell* **176**, 1174–1189 (2019).

48. J. G. White, E. Southgate, J. N. Thomson, S. Brenner, The structure of the nervous system of the nematode *Caenorhabditis elegans. Philos. Trans. R. Soc. Lond. B Biol. Sci.* **314**, 1–340 (1986).

49. S. Maslov, K. Sneppen, Specificity and stability in topology of protein networks. *Science* **296**, 910–913 (2002).

50. P. Liu *et al.*, Six innexins contribute to electrical coupling of *C. elegans* body-wall muscle. *PloS One* **8**, e76877 (2013).

51. C. F. Chuang, M. K. VanHoven, R. D. Fetter, V. K. Verselis, C. I. Bargmann, An innexin-dependent cell network establishes left-right neuronal asymmetry in *C. elegans. Cell* **129**, 787–799 (2007).

52. A. Oshima, T. Matsuzawa, K. Nishikawa, Y. Fujiyoshi, Oligomeric structure and functional characterization of *Caenorhabditis elegans* innexin-6 gap junction protein. *J. Biol. Chem.* **288**, 10513–10521 (2013).

53. T. C. Südhof, Towards an understanding of synapse formation. *Neuron* **100**, 276–293 (2018).

54. C. S. Xu *et al.*, A connectome of the adult *Drosophila* central brain. bioRxiv:911859 (21 January 2020).

55. K. Eichler *et al.*, The complete connectome of a learning and memory centre in an insect brain. *Nature* **548**, 175–182 (2017).

56. K. Davie *et al.*, A single-cell transcriptome atlas of the aging *Drosophila* brain. *Cell* **174**, 982–998 (2018).

57. D. G. C. Hildebrand *et al.*, Whole-brain serial-section electron microscopy in larval zebrafish. *Nature* **545**, 345–349 (2017).

58. M. Tambalo, R. Mitter, D. G. Wilkinson, A single cell transcriptome atlas of the developing zebrafish hindbrain. *Development* **147**, dev184143 (2020).

59. G. Cimini *et al.*, The statistical physics of real-world networks. *Nat. Rev. Phys.* **1**, 58–71 (2019).

60. T. Squartini, G. Caldarelli, G. Cimini, A. Gabrielli, D. Garlaschelli, Reconstruction methods for networks: The case of economic and financial systems. *Phys. Rep.* **757**, 1–47 (2018).

61. S. M. O'Rourke *et al.*, A survey of new temperature-sensitive, embryonic-lethal mutations in *C. elegans*: 24 alleles of thirteen genes. *PloS One* **6**, e16644 (2011).

62. S. Li, J. A. Dent, R. Roy, Regulation of intermuscular electrical coupling by the *Caenorhabditis elegans* innexin inx-6. *Mol. Biol. Cell* **14**, 2630–2644 (2003).

63. N. Sahni *et al.*, Widespread macromolecular interaction perturbations in human genetic disorders. *Cell* **161**, 647–660 (2015).

64. G. H. Golub, M. Heath, G. Wahba, Generalized cross-validation as a method for choosing a good ridge parameter. *Technometrics* **21**, 215–223 (1979).

65. S. Chatterjee *et al.*, Random graphs with a given degree sequence. *Ann. Appl. Probab.* **21**, 1400–1435 (2011).